Organic Process Research & Development **2010,** *14,* 393–404

ReactIR Flow Cell: A New Analytical Tool for Continuous Flow Chemical Processing

Catherine F. Carter,[†] Heiko Lange,[†] Steven V. Ley,*[,†] Ian R. Baxendale,[†] Brian Wittkamp,[‡] Jon G. Goode,[§] and Nigel L. Gaunt[§]

Innovative Technology Centre, Department of Chemistry, University of Cambridge, Lensfield Road, Cambridge CB2 1EW, U.K., Mettler-Toledo AutoChem, 7075 Samuel Morse Drive, Columbia, Maryland 21046, U.S.A., Mettler-Toledo AutoChem UK, 64 Boston Road, Beaumont Leys, Leicester LE4 1AW, UK

Abstract:

A newly developed ReactIR flow cell is reported as a convenient and versatile inline analytical tool for continuous flow chemical processing. The flow cell, operated with ATR technology, is attached directly into a reaction flow stream using standard OmniFit (HPLC) connections and can be used in combination with both meso- and microscale flow chemistry equipment. The iC IR analysis software (version 4.0) enables the monitoring of reagent consumption and product formation, aiding the rapid optimisation of procedures. Short-lived reactive intermediates can also be observed *in situ*, giving further mechanistic insight into complex transformations.

1. Introduction

Advanced chemical processing techniques that facilitate an optimum use of resources are important in order to further streamline chemical procedures. Making the most efficient use of substrates, solvents, energy, and the working hours of skilled practical chemists is desirable in terms of time management and laboratory efficiency.[1] Modern continuous flow reactor technologies provide the opportunity to address many of these issues as they allow for rapid testing, optimisation, and scaling of chemical sequences, often giving more efficient reaction profiles that make use of higher temperature and pressure tolerances.[2] Another important component is the high reliability of these methods which ensures precise reaction control, thereby minimising the formation of undesired byproducts which are costly to separate or recycle.[2] This aspect is particularly relevant for reactions in which toxic or hazardous byproducts are generated.[3] For a number of years, our group has been exploring methods to assist chemical synthesis with a focus on developing flow chemistry platforms.[4] However, an often limiting factor with these methods relates to inline monitoring as this would be of importance with respect to optimisation and synchronised control of ongoing reactions.

One of the most convenient and nondestructive methods for real-time inline monitoring is infrared (IR) spectroscopy. This approach has found application in a number of scenarios[5] but has often employed bespoke flow-through IR cells based upon ATR technology.[6] Despite being successful for their designed application, these tools have suffered from a lack of integration and convenient software control and therefore have not provided a generic solution across all platforms. We therefore recognised the need to enter into a collaboration with a suitable expert manufacturer to develop a robust and versatile unit capable of operating across research and process environments where flow chemistry is practiced.[7] Our preliminary attempt to achieve this goal has been reported earlier this year[8] using a commercially available fibre-optic cable fitted with an FT-IR diamond flow probe. We have now substantially improved and refined the flow cell which can now be readily operated directly linked to a ReactIR 45m instrument[7] (Figure 1). With this new opportunity for inline analytical monitoring, we aimed to investigate and solve some of the most challenging issues concerning the optimisation and synchronised control of continuous chemical processing as it stands today. These namely include:

- Monitoring (and quantisation) of dispersion, worsened by diffusion. Major problems arise thereof as predictions concerning how long it takes for the bulk of the product to exit the flow reactor system are often unreliable. Although dispersion curves can be calculated based on

* Author for correspondence. E-mail: svl1000@cam.ac.uk.
[†] Innovative Technology Centre, University of Cambridge.
[‡] Mettler-Toledo AutoChem, U.S.A.
[§] Mettler-Toledo AutoChem, UK.

(1) See for example: (a) Li, C.-J.; Trost, B. M. *Proc. Natl. Acad. Sci. U.S.A.* **2008**, *105*, 13197–13202, and literature cited therein. (b) Wender, P. A.; Verma, V. A.; Paxton, T. J.; Pillow, T. H. *Acc. Chem. Res.* **2008**, *41*, 40–49.

(2) Selected reviews on the concept, the benefits, the applications and the tools of flow chemistry: (a) Mak, X. Y.; Laurino, P.; Seeberger, P. H. *Beilstein J. Org. Chem.* **2009**, *5*, No. 19.; 10.3762/bjoc.5.19. (b) Teh, S. Y.; Lin, R.; Hung, L. H.; Lee, A. P. *Lab Chip* **2008**, *8*, 198–230. (c) Wilms, D.; Klos, J.; Frey, H. *Macromol. Chem. Phys.* **2008**, *209*, 343–356. (d) Singh, B. K.; Kaval, N.; Tomar, S.; Van der Eycken, E.; Parmar, V. S. *Org. Process Res. Dev.* **2008**, *12*, 468–474. (e) Wiles, C.; Watts, P. *Eur. J. Org. Chem.* **2008**, 1655–1671. (f) Mason, P. B.; Proce, K. E.; Steinbacher, J. L.; Bogdan, A. R.; McQuade, D. T. *Chem. Rev.* **2007**, *107*, 2300–2318. (g) Baxendale, I. R.; Ley, S. V. *Solid Supported Reagents in Multi-Step Flow Synthesis in Ernst Schering Foundation Symposium Proceedings*; Seeberger, P. H., Blume, T., Eds.; Springer-Verlag: Berlin, Heidelberg, 2007; Vol. 3, pp 151−185. (h) Kirschning, A.; Solodenko, W.; Mennecke, K. *Chem. Eur. J.* **2006**, *12*, 5972–5990. (i) *Chemical Micro Process Engineering: Processing and Plants*; Hessel, V., Löwe, H., Müller, A., Kolb, G., Eds.; Wiley-VCH: Weinheim, 2005. (j) Hodge, P. *Ind. Eng. Chem. Res.* **2005**, *44*, 8542–8553. (k) Lee, C. K. Y.; Holmes, A. B.; Ley, S. V.; McConvey, I. F.; Al-Duri, B.; Leeke, G. A.; Santos, R. C. D.; Seville, J. P. K. *J. Chem. Soc., Chem. Commun.* **2005**, 2175–2177. (l) Jas, G.; Kirschning, A. *Chem. Eur. J.* **2005**, *9*, 5708–5723. (m) Doku, G. N.; Verboom, W.; Reinhoudt, D. N.; van den Berg, A. *Tetrahedron* **2005**, *61*, 2733–2742. (n) Jas, G.; Kirschning, A. *Chem. Eur. J.* **2003**, *9*, 5708–5723. (o) Hafez, A. M.; Taggi, A. E.; Lectka, T. *Chem. Eur. J.* **2002**, *8*, 4114–4119. (p) *Microreactors: New Technology for Modern Chemistry*; Ehrfield, W., Hessel, V., Löwe, H., Eds.; Wiley-VCH: Weinheim, 2000. (q) Hafez, A. M.; Taggi, A. E.; Wack, H.; Drury, W. J.; Lectka, T. *Org. Lett.* **2000**, *2*, 3963–3965.

(3) Of special interest in this respect are, for example: azide sources (see ref 19), ozone (see ref 5a), diazomethane (Martin, L. J.; Ley, S. V. University of Cambridge, UK. Unpublished work, 2009), fluoride sources (see ref 10).

10.1021/op900305v
Published on Web 02/01/2010

Figure 1. **ReactIR 45m with prototype of IR flow cell attached. (a) Flow cell in line, connected with OmniFit adapters; (b) flow cell with OmniFit adapters removed, with direction of flow stream through the cell indicated; (c) head unscrewed, free view on diamond window (arrow).**

model systems, arbitrary differences to real systems cause problems in multistep sequences as it makes it difficult to synchronise a third stream of reagents, particularly with challenging 1:1 stoichiometry.

- Inline (real-time) monitoring. This can not be achieved in a closed system without taking a sample and analysing it off-line.
- Inline monitoring of products and intermediates without chemically transforming them, as well as analysis within rapid screening processes. This affords a precise and fast analytical method which provides the result within seconds. UV detectors commonly used so far often suffer from a lack of specificity.
- Hazardous compounds representing an additional challenge in flow. Although we have improved safety profiles by working in contained systems with only small amounts at any one time, it would be beneficial if one could monitor the levels of these substances with an inline detection method.
- Permanent qualitative monitoring of product formation on a large scale. This quality-control application could ideally aid in synchronising multiple reaction streams.

In this technical report we now describe on the basis of selected experiments how the new analytical FT-IR tool can be used to conveniently overcome the issues listed above.

2. Technical Details

The FT-IR device used in this work is a ReactIR 45 m fitted with a 24 h mercury cadmium telluride (MCT) detector. The ReactIR instrument was directly connected to a newly developed, microscale flow cell (Figure 1). The flow cell comprises of an integrated attenuated total reflectance (ATR) gold sealed diamond sensor (referred to as DiComp) that allows *in situ*, real-time monitoring of a continuous flow stream. The full infrared spectral region is available with this micro flow cell (650−1950 cm^{-1} and 2250−4000 cm^{-1}) excluding the diamond "blind spot" which only allows very weak absorbance in this region, outlined in Figure 2. The IR flow cell has a removable head allowing for easy cleaning (Figure 1c) and an internal volume of 51 μL. It can be heated up to 60 °C using an external controller, and it can be operated up to 30 bar pressure. OmniFit connections (1/4-28) enable the IR flow cell to be easily incorporated into any continuous flow chemical processing setup.

An integrated resistive thermal device (RTD) temperature sensor is also built into the cell in order to track its temperature, paying deference to the fact that the IR spectroscopy is a temperature-dependent spectroscopy. While the flow stream is running through the cell, scans are taken at predefined intervals. The system is controlled and the raw data are collected and analysed by the iC IR reaction analysis software (version 4.0).[7]

3. General Remarks on Setups and Procedures

To test the new IR flow cell in combination with the ReactIR 45m and the iC IR software we designed a set of representative flow chemistry experiments to tackle some of the challenges

(4) Selected recent applications of flow chemistry: (a) Sedelmeier, J.; Schou, S. C.; Ley, S. V.; Baxendale, I. R. *Chem. Eur. J.* **2010**, *6*, 89−94. (b) Palmieri, A.; Ley, S. V.; Hammond, K.; Polyzos, A.; Baxendale, I. R. *Tetrahedron Lett.* **2009**, *50*, 3287–3289. (c) Baxendale, I. R.; Ley, S. V.; Mansfield, A. C.; Smith, C. D. *Angew. Chem.* **2009**, *121*, 4071–4081. *Angew. Chem., Int. Ed.* **2009**, *48*, 4017−4021. (d) Sedelmeier, J.; Ley, S. V.; Lange, H.; Baxendale, I. R. *Eur. J. Org. Chem.* **2009**, 4412–4420. (e) Baumann, M.; Baxendale, I. R.; Ley, S. V.; Nikbin, N.; Smith, C. D. *Org. Biomol. Chem.* **2008**, *6*, 1587–1593. (f) Smith, C. J.; Iglesias-Sigüenza, F. J.; Baxendale, I. R.; Ley, S. V. *Org. Biomol. Chem.* **2007**, *5*, 1562–1568. (g) Vickerstaffe, E.; Villard, A.-L.; Ladlow, M.; Ley, S. V. *Synlett* **2007**, 1251–1254. (h) Baxendale, I. R.; Deeley, J.; Griffiths-Jones, C. M.; Ley, S. V.; Saaby, S.; Tranmer, G. K. *Chem. Commun.* **2006**, 2566–2568. (i) Saaby, S.; Knudsen, K. R.; Ladlow, M.; Ley, S. V. *Chem. Commun.* **2005**, 2909–2911.

(5) Selected publications on inline IR spectroscopy and closely related topics: (a) Hübner, S.; Bentrup, U.; Budde, U.; Lovis, K.; Dietrich, T.; Freitag, A.; Küpper, L.; Jähnisch, K. *Org. Process Res. Dev.* **2009**, *13*, 952–960. (b) Trevisan, M. G.; Poppi, R. J. *Talanta* **2008**, *75*, 1021–1027. (c) Trevisan, M. G.; Garcia, C. M.; Schuchardt, U.; Poppi, R. J. *Talanta* **2008**, *74*, 971–976. (d) Nair, S. A.; Nozaki, T.; Okazaki, K. *Ind. Eng. Chem. Res.* **2007**, *46*, 3486–3496. (e) Koster, G.; Huh, J.-U.; Hammond, R. H.; Beasley, M. R. *Appl. Phys. Lett.* **2007**, *90*, 261917. (f) Muthusamy, M.; Burrell, M. R.; Thorneley, R. N. F.; Bornemann, S. *Biochemistry* **2006**, *45*, 10667–10673. (g) Kaun, N.; Kulka, S.; Frank, J.; Schade, U.; Vellekoop, M. J.; Haraseke, M.; Lendl, B. *Analyst* **2006**, *131*, 489–494. (h) Haberkorn, M.; Hinsmann, P.; Lendl, B. *Analyst* **2002**, *127*, 109–113. (i) Colston, B. J.; Choppin, G. R.; Taylor, R. J. *Radiochim. Acta* **2000**, *88*, 329–334. (j) Suga, S.; Okajima, M.; Fujiwara, K.; Yoshida, J. *J. Am. Chem. Soc.* **2001**, *123*, 7941–7942. (k) MacLaurin, P.; Crabb, N. C.; Wells, I.; Worsfold, P. J.; Coombs, D. *Anal. Chem.* **1996**, *68*, 1116–1123. (l) Banister, J. A.; Howdle, S. M.; Poliakoff, M. *J. Chem. Soc., Chem. Commun.* **1993**, 1814–1815. (m) Olesik, S. V.; French, S. B.; Novotny, M. *Anal. Chem.* **1986**, *58*, 2256–2258.

(6) An ATR technology based IR flow cell specially tailored for analysing aqueous solutions is available from Bruker Optik GmbH Rudolf-Plank-Strasse 27, 76275 Ettlingen, Germany. Website: www.brukeroptics.com.

(7) (a) The ReactIR 45m and the reaction analysis software iC IR 4.0 are available from Mettler-Toledo AutoChem, 7075 Samuel Morse Drive, Columbia, Maryland, U.S.A. Webinars are available detailing the use of these two previously launched parts of the analytical tool described in here; website: www.mt.com. (b) The IR flow cell can be easily replaced by the conventional fibre-optic probe arm as necessary (and *vice versa*). This exchange needs to be accompanied by selecting the probe-specific preadjustments within the software rather than the IR flow cell-specific set of preadjustments.

(8) (a) Carter, C. F.; Baxendale, I. R.; O'Brien, M.; Pavey, J. B. J.; Ley, S. V. *Org. Biomol. Chem.* **2009**, *7*, 4594–4597. (b) Carter, C. F.; Baxendale, I. R.; Pavey, J. B. J.; Ley, S. V. *Org. Biomol. Chem.* **2009**, *7*, in press.

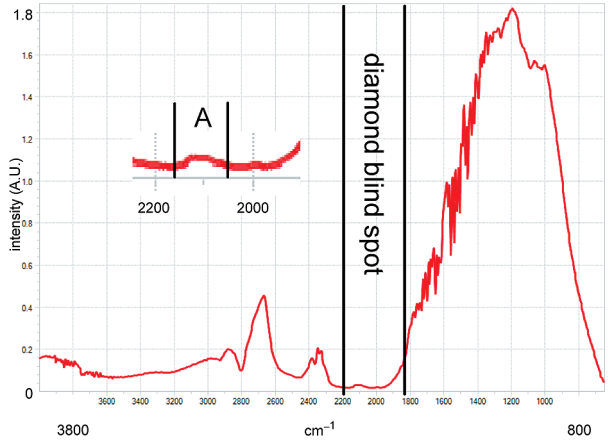

Figure 2. **Background spectrum of air showing the diamond blind spot and the small area A which allows for some absorbance within this region.**

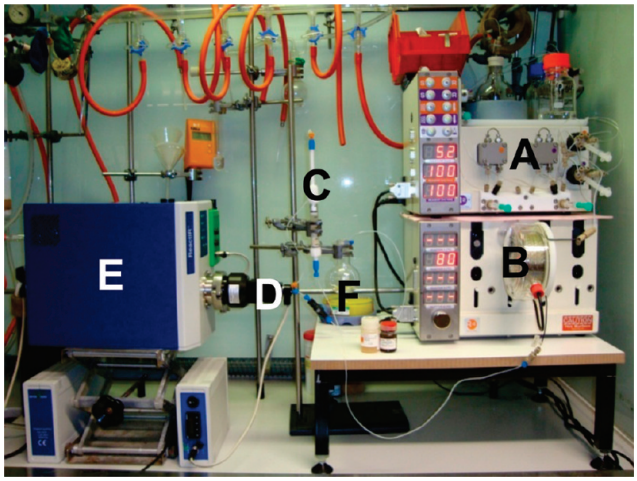

Figure 3. **Exemplary setup for monitoring the product formation within a continuous flow processing using the Vapourtec R2+/R4 flow chemistry system[9] (vide infra for experiment). Legend: (A) R2+ double pump unit. (B) R4 unit with CFC reactor connected. (C) OmniFit column filled with polymer-supported scavenger. (D) MT IR flow cell. (E) ReactIR 45m. (F) Flask containing product solution.**

connected with flow chemistry (*vide supra*). In this series of evaluation experiments we used some of the most common continuous flow chemistry platforms and coupled them to the new inline IR device. However, before discussing the results, certain general comments on reaction setups and procedures used are pertinent:

- The IR flow cell can be attached inline at any point of the flow reaction setup, depending on the issue that needs to be addressed (monitoring product formation, monitoring intermediates, etc.). However, owing to the design of the initial IR flow cell we found that better results were obtained when the flow cell is accompanied by a back-pressure regulator. This should be attached inline after the flow cell in order to prevent cell drainage in those cases where the IR flow cell is the last piece of equipment. An exemplary setup is shown in Figure 3.
- After collecting a background spectrum of air (Figure 2) it is wise to create an initial library of the IR spectra of the compounds under study since this greatly aids analysis and provides details of the best choice of absorption bands for the monitoring process. This is carried out by injecting standard solutions of those compounds in the reaction solvent at the reaction concentration into the cell using a syringe adapter. Having a good library of compounds also assists in the analysis of unknown intermediates or compounds occurring in the reactions.
- Once the raw experimental data have been collected, the iC IR software is used to analyse and, if necessary, mathematically manipulate the raw data. Using peak monitoring features it is possible to select specific known or previously unknown wavenumbers to follow throughout the reaction; this can be done simultaneously and even in retrospect if necessary. This feature allows for the generation of trend graphs by examining changes in absolute peak intensity over time (absolute scale, measured in absorbance units (AU)), or for comparison of trends from different compounds (relative scales, given in %).

Scheme 1. **Fluorination reaction in flow using DAST[10]**

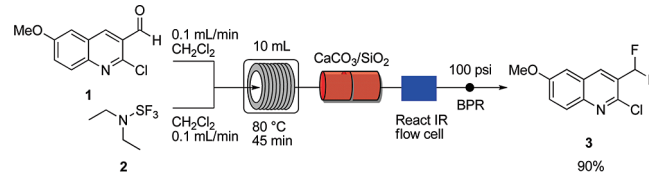

Although not studied in this work, it is in principle possible to delineate quantitative information from the data obtained by the ReactIR 45m flow cell measurements by performing an upstream calibration of the instrument.

4. Results and Discussion

4.1. Monitoring Product Streams and Their Dispersion.

Firstly we used the IR flow cell to gain information about product dispersion. We reproduced three reliable flow procedures with the new IR flow cell attached inline at the end of the reaction stream.

4.1.1. Fluorination Reactions Using DAST. Previously we have used the Vapourtec R2+/R4 flow chemistry system[9] in combination with solid-supported reagents and scavengers to perform fluorination reactions in a continuous fashion (Scheme 1).[10] The fluorination reaction itself takes place inside the convection heated flow coil (CFC), while the $CaCO_3$ and SiO_2 column provides an inline quench and cleanup.

The region where C−F bonds are expected to absorb was monitored during the reaction (Figure 4), enabling a trend based on the peak intensity to be produced. The clear appearance of the product C−F at $\tilde{\nu} = 1201\ cm^{-1}$ was noted after 65 min (Figure 5). Further, the effectiveness of the silica gel column at scavenging any unreacted aldehyde **1** is demonstrated (Figure 4b, red line), as no absorbance is seen in the carbonyl region that was being monitored relative to the background spectra of this reagent.

(9) Vapourtec R2+ and R4 units are available from Vapourtec Ltd., Place Farm, Ingham, Suffolk IP31 1NQ, UK. Website: www.vapourtec.co.uk.

(10) (a) Baumann, M.; Baxendale, I. R.; Martin, L. J.; Ley, S. V. *Tetrahedron* **2009**, *65*, 6611–6625. (b) Bluck, G. W.; Ley, S. V. University of Cambridge, UK. Unpublished work, 2009. (c) Baumann, M.; Baxendale, I. R.; Ley, S. V. *Synlett* **2008**, 2111–2114.

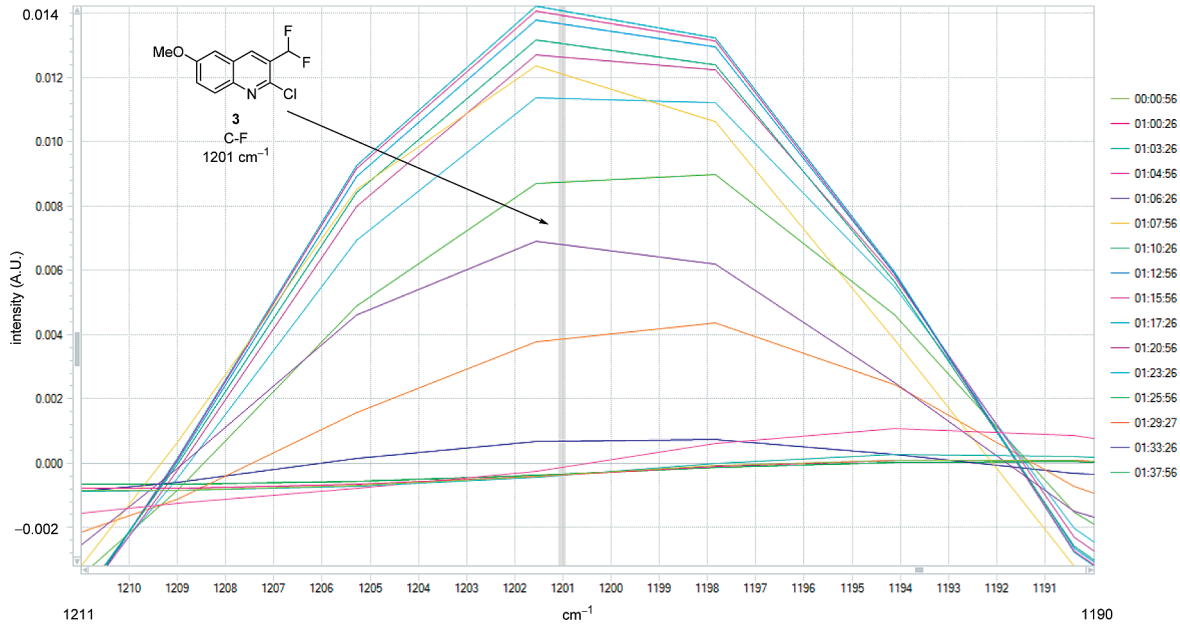

Figure 4. **Fluorination of aldehyde 1: detailed view of selected raw spectra (second derivative) indicating the rise and decay in peak height.**

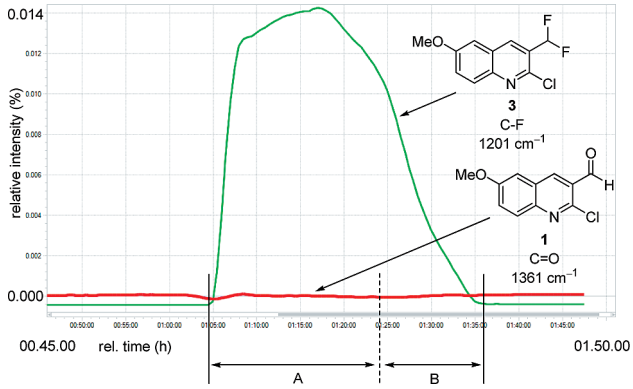

Figure 5. **Trends based upon peak height analysis, displaying the dispersion information obtained by the IR flow cell within the fluorination of 1.**

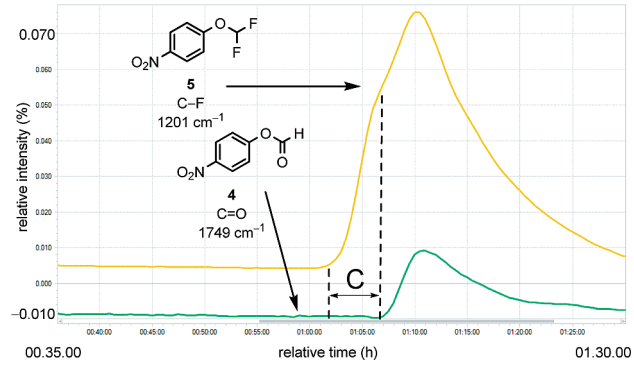

Figure 6. **Monitoring chromatographic effects within the fluorination of ester 4 in flow (time delay C between the commencing exit of the two compounds out of the flow stream).**

The shape of the trend curve arises from the dispersion effect mentioned earlier (Figure 5). The expected time for the product to pass through the cell is 20 min (A), calculated from the volume of material injected and the flow rate at which it is being pumped (4 mL at 0.2 mL/min = 20 min). The extra 16 min (B) is due to dispersion, diffusion, and chromatographic effects caused by the reaction setup. This is very informative because, if a third stream were to be added to the output from this reaction, it is essential to operate the third pump at a specific flow rate so that the new reagent can react with all 36 min worth of product stream.

We then examined a similar fluorination of ester **4**, which is a more challenging substrate that had not been previously reported in the literature (Scheme 2).

Scheme 2. **Fluorination of ester 4 using DAST**

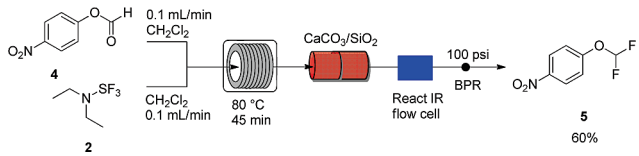

The informative observation in this experiment (apart from monitoring the product dispersion) was the time delay between the appearance of the product and the remaining unreacted starting material (ester **4** was not expected to be scavenged by the cleanup column) in the IR flow cell (Figure 6). This time delay of 5 min for its appearance in the flow cell represents the chromatographic effect of having the silica gel column inline.

Using this information it should be possible, for example, to extend the length of the silica gel column inline to achieve a separation of the product from the starting material by means of chromatography; i.e. performing flash column chromatography inline.

4.1.2. Oxazole Formation. A similar reaction arrangement was employed for the formation of oxazole **8** from isocyanide **7** and acid chloride **6**, of which the detailed experimental conditions have been reported earlier (Scheme 3).[11] In this experiment we were unfortunately not able to monitor the N≡C stretch of the isocyanide as it absorbs in the $\tilde{\nu}$ = 1950−2250

(11) Baumann, M.; Baxendale, I. R.; Ley, S. V.; Smith, C. D.; Tranmer, G. K. *Org. Lett.* **2006**, *8*, 5231–5234.

Scheme 3. **Flow synthesis of oxazole 8**

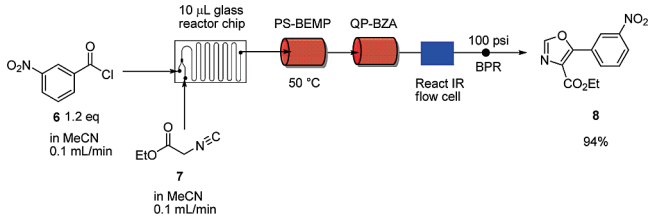

cm^{-1} region which is desensitised by the diamond absorption of the cell (compare Figure 2).[12]

Nevertheless, monitoring the product output from the formation of oxazole **8** was possible by using the ester carbonyl bands since the wavenumber corresponding to the conjugated ester in the product **8** ($\tilde{\nu} = 1721\ cm^{-1}$) was significantly different from that in the original isocyanide **7** ($\tilde{\nu} = 1760\ cm^{-1}$) (Figure 7). These results also show the effectiveness of the column of benzylamine as a scavenger for removing the surplus acid chloride that is used in excess to drive the reaction to completion (Scheme 3). The shape of the graph contains additional information when compared with the earlier fluorination reactions. In this case, 4 mL of material is pumped at 0.4 mL/min, but still requires 30 min for full collection of product. Consequently, it can be seen that the addition of a second scavenging column significantly contributes to the dispersion of the exiting reaction stream.

These first examples clearly demonstrate that the cell can be readily integrated into a typical flow chemistry experimental setup and used to monitor product streams, giving essential information concerning dispersion and the effectiveness of the scavenging systems employed. Up to now, the only way of obtaining similar information was *via* UV detection, which is inappropriate for a large number of compounds and has insufficient specificity in general. With the new IR flow cell system, multiple wavenumbers can be monitored simultaneously inline, allowing unreacted starting materials to be distinguished from products.

4.2. Real-Time Reaction Monitoring. In these examples, the IR flow cell is attached inline in order to gain information about the real-time progress of a reaction in a closed flow system. Typically a sample would have to be taken offline to achieve this. A recycling protocol was established to attempt reaction monitoring with minimal disruption to the continuous process.

4.2.1. Hydrogenation Reactions. The ability to continuously monitor hydrogenation reactions *in situ* is highly desirable, owing to catalyst variation which can lead to inconsistent reaction times or conversions. Using the commercially available hydrogenation flow reactors H-Cube and H-Cube Midi,[13] a reaction setup was designed to incorporate the IR flow cell without exposing it to the high temperatures and pressures sometimes required in these transformations (Figure 8). The

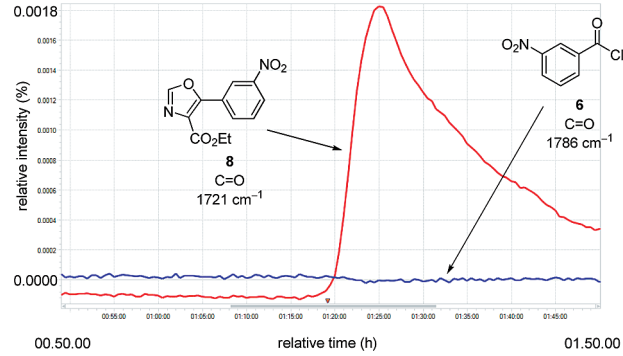

Figure 7. **Trend curves obtained within the formation of oxazole 8; exponential flattening out of the red trend curve not shown.**

reaction mixture was therefore withdrawn through the cell into the pump head, prior to entering the hydrogenation reactor, and back into the same flask (Figure 8).

The full saturation of nicotinate **9** on a 5 g scale was chosen as a suitable process for study using the H-Cube Midi (Figure 8).[14] This experiment would enable us to test the performance of the IR flow cell under fast flow rates (5 mL/min) and also to investigate whether meaningful information could be obtained from a reaction carried out in a solvent mixture which exhibits very strong absorption itself.

As hydrogenations are typically performed at high dilution, a concentration screen was performed to ascertain the minimum concentration at which the different bands in the starting material could be monitored (Figure 9).

As can be seen in Figure 9, measurable information could still be obtained at 0.01 M using the solvent subtraction feature in the software. However, the ester carbonyl could be monitored at very low concentrations even without solvent subtraction (due to an easier monitoring of strong absorption bands at lower concentrations), whereas absorptions of more weakly absorbing bands such as the C═C require higher concentrations in general.

The reaction itself was finally operated at 0.1 M with a 5 mL/min flow rate, and the gradual disappearance of the C═C bond was monitored. The appearance of the saturated ester band was also distinguished from the disappearance of the absorption for the conjugated ester (Figure 10). This demonstrates that it is beneficial to have more than one point of structural reference in the same molecule to validate the results, particularly for weak bands at high temperature.

It further appears that the reaction setup itself seems to create a not yet fully understood spiking phenomenon in the output trend curves; nevertheless a consistent trend can be observed giving valuable and rapid information on the reaction progress.

Cross-validating these findings we performed a small-scale hydrogenation experiment. This time the H-Cube was used in combination with the flow cell; again, a recycling process was run. Butane-2,3-diacetal (BDA) protected alkene **11**, which was synthesised as described earlier,[8] is transformed to *meso* compound **12** via hydrogenation using a Rh/Al_2O_3 catalyst (Scheme 4).

(12) We are currently awaiting a number of third-generation IR flow cells. These include a diamond-based flow cell with improved optics, a silicon-based flow cell, a double-headed IR flow cell, and a flow cell with 10 μL head volume. These cells will be thoroughly tested in due course. The results will be compared to the results obtained with the prototype.

(13) The H-Cube and the H-Cube Midi are available from ThalesNano, Inc.,Gázgyaru.1-3,Budapest,HungryH-1031.Website:www.thalesnano.com.

(14) (a) Moon, M. S.; Lee, S. H.; Cheong, C. S. *Bull. Korean Chem. Soc.* **2001**, *22*, 1167–1168. (b) Liljeblad, A.; Kavenius, H.-M.; Taehtinen, P.; Kanerva, L. T. *Tetrahedron: Asymmetry* **2007**, *18*, 181–191.

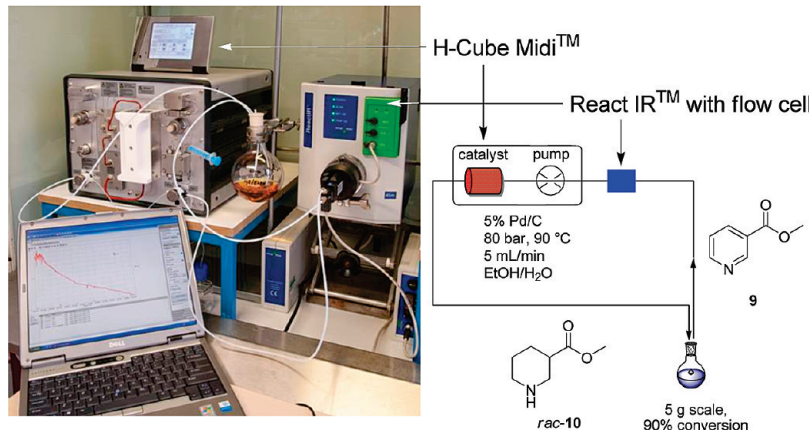

Figure 8. **Setup for monitoring flow hydrogenation with the IR flow cell using a recycling process.**

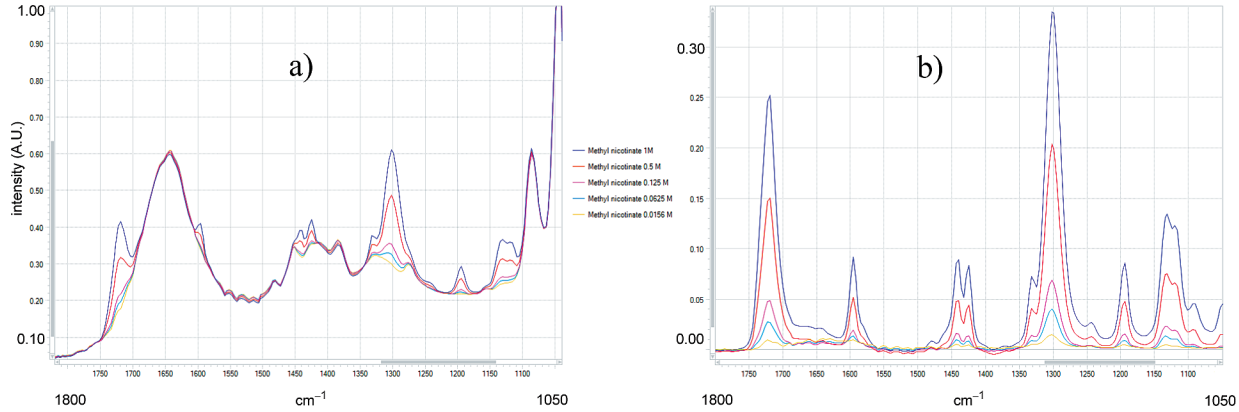

Figure 9. **IR flow cell detection limit screen: (a) Raw data. (b) Spectra obtained after solvent subtraction (40% EtOH/H_2O).**

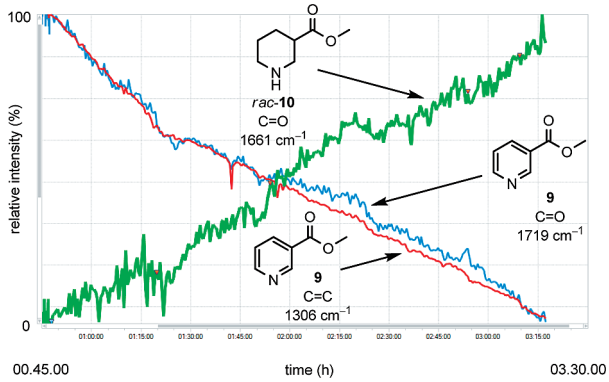

Figure 10. **Multiple band monitoring within the heterocycle saturation reaction.**

Scheme 4. **Recycling process for the hydrogenation of BDA-derivative 11 using the H-cube®**

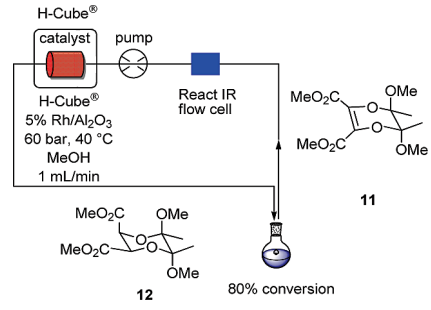

Figure 11 shows a section of the raw data that was collected from the flow cell in real-time. The disappearance of the alkene band at $\tilde{\nu} = 1652$ cm^{-1} is clearly visible. However, when the reaction appeared complete according to the IR spectrum, the conversion by ^{1}H NMR was just 80%. This observation represents the level at which the very weak band for the alkene diminishes into the baseline noise of the spectrum.[12] However, when extrapolating the trend curves, the time needed for a conversion >95% can be estimated.

4.3. Screening of Reaction Conditions. Up to this point the IR flow cell has been used principally for product monitoring during continuous flow synthesis. We envisaged that the IR flow cell could be used for very rapid qualitative screening purposes to quickly obtain trends against reaction parameters. This could dramatically reduce the time required to optimise a procedure because a general trend could be obtained in a single setup.

4.3.1. Butane-2,3-diacetal Protection. The BDA protection of chloropropane diol **13** was chosen as a platform to investigate the screening properties of the IR flow cell (Scheme 5).

The reagents were continuously pumped through the CFC reactor as the temperature was systematically increased while monitoring the signal intensity of the C−O ether bond in the product. As expected a direct increase in product formation with temperature was observed (Figure 12). Making use of the flow reactor arrangement screening of multiple temperatures in just one reaction setup is possible and provides good qualitative data towards the ideal reaction condition by rapid profile mapping. We were pleased to find that this profile mapping corresponded to the one obtained earlier[8] using several batch reactions. It is possible to gain quantitative information using the software;

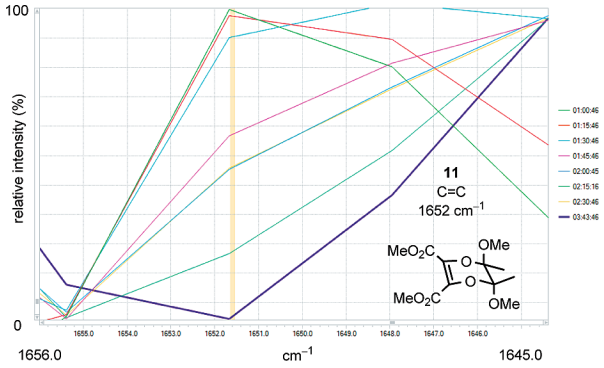

Figure 11. **Disappearance of the alkene C═C band at $\tilde{\nu} = 1652$ cm^{-1} over time.**

Scheme 5. **BDA protection of halopropanediol 13**

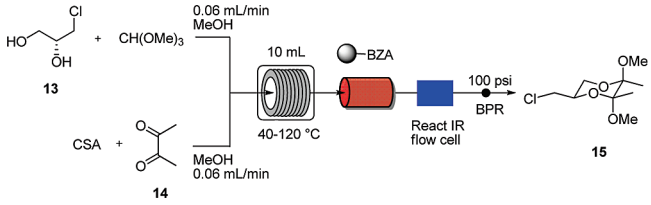

this requires calibration procedures of the peak heights against yields/conversions.

As we need large quantities of these BDA-derivatives for our ongoing research, we decided to use the IR flow cell to monitor the product formation during a scale-up experiment, in which the reactor was operated for 24 h. The trend curve obtained is shown in Figure 13. The IR flow cell could easily monitor the formation over the longer period of time, and it indicated two reactor failures during this 24 h period, after ~2.5 h and after ~4.25 h. Bearing in mind that there is a monitoring delay of approximately 100 min due to the reaction setup (30 mL CFC-reactor, 0.3 mL/min total flow rate), the second drop in peak intensity can be understood by an indicated reactor failure which coincidently occurred around the time when the first intensity drops where recorded. However, these first fluctuations in the product formation must be due to an event approximately 100 min before, which remained unnoticed by the reactor itself and which therefore would have completely remained unnoticed without the IR flow cell.

4.3.2. Marshall's Chemistry in Microscale Flow Mode. As the investigation of low temperature reactions in flow mode is

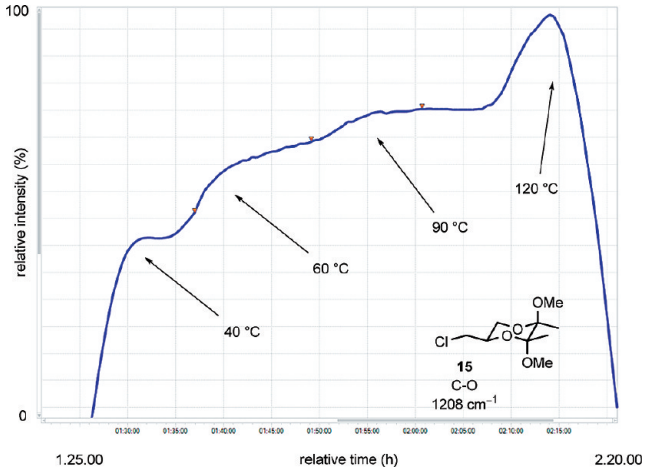

Figure 12. **Temperature screening with the IR flow cell.**

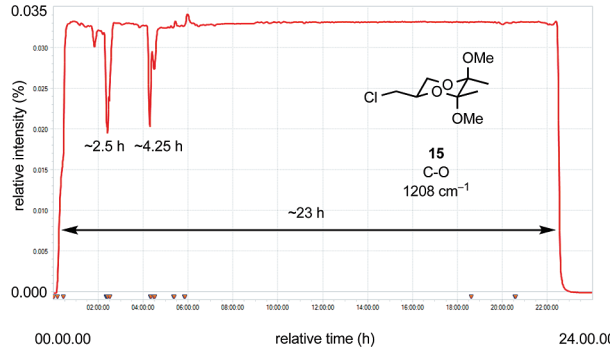

Figure 13. **Trend curve obtained for a 24 h long-term production of BDA derivative 15 indicating two reactor failures in the first six hours.**

Scheme 6. **Screening setup for the chain elongation according to the Marshall protocols**

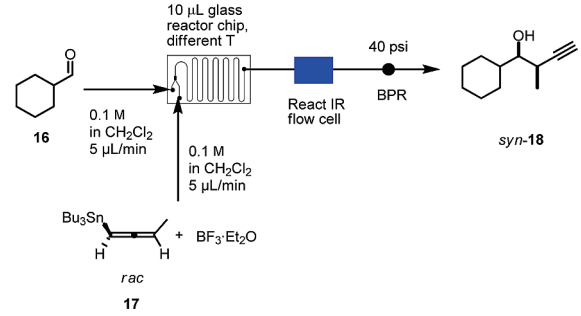

of particular interest to our group, among these the diastereoselective chain elongation according to Marshall's protocols (Scheme 6),[15,16] we further validated the screening capabilities of the IR flow cell at a significantly reduced scale using a microfluidic reaction platform. The IR flow cell was attached to the exit of a 10 μL glass reactor chip.[17] Performing the desired screening on that scale would also enable us to test whether the cell can monitor very fast reaction processes.

Using the general arrangement shown in Scheme 6 a temperature screen, using a Peltier heating block, and a residence time screen, using a set of twin syringe pumps, were performed. All components of the reaction could be independently monitored, namely the product acetylene **18**, the starting allene **17** and the aldehyde **16**. The deconvoluted IR band trends obtained (Figure 14) indicate two important facts: first, the product formation is robust at 0 °C, second, the reaction itself

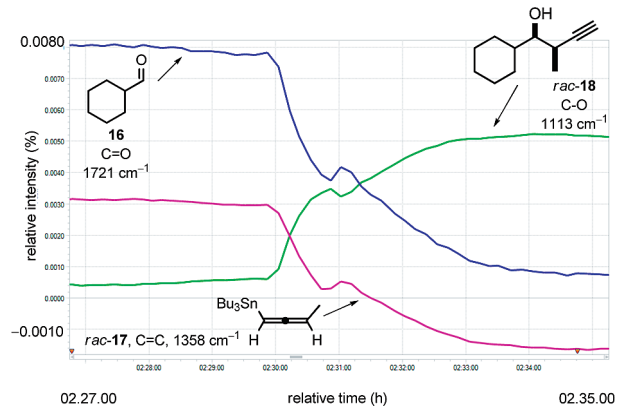

Figure 14. **Detail view of the trend curves showing rapid product formation within the microscale screening procedure for the chain elongation according to the Marshall protocols.**

Scheme 7. **Curtius rearrangement in flow with temperature screening**

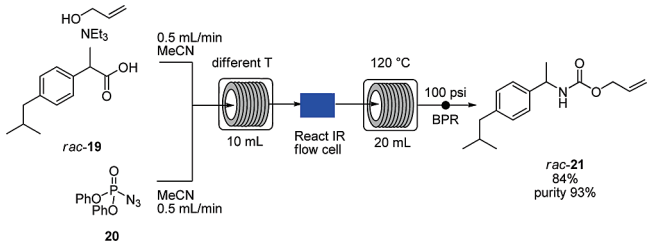

is much faster than originally expected based on initial batch observations. The total residence time of the reaction mixture in the cooled 10 μL glass reactor chip amounted to approximately only one minute prior to entering the IR flow cell. In this way, it was possible to accurately monitor a vast range of reaction conditions using minimal material, with a single reliable analytical device and thereby map out a large reaction data field. The optimal conditions found by this screening process could then be successfully transferred to a mesoscale reactor for scale-up.

In this work there is an issue concerning the currently available volume of the prototype flow cell (51 μL) which is five times larger than the 10 μL volume of the reaction chip.[12] The consequence of this mismatch is an intrinsic time delay between any chemical change and the IR monitoring of the effect, so the trends have to be viewed accordingly.

These results clearly demonstrate the benefits of applying an inline monitoring device for screening since the whole experimental sequence was conducted in only 3.5 h in total, including the setting up of the apparatus, monitoring of the reaction, and the cleaning of the devices for the next series of experiments. The results we obtained rapidly afforded the best conditions by delivering the highest amount of product with minimal formation of byproduct.[15]

4.4. Monitoring Reactive Intermediates. One major advantage of flow chemistry that we have demonstrated previously is the ability to generate reactive and hazardous intermediates inline and to then react them further *in situ*. Final products can finally be obtained free from potentially dangerous components. A unique opportunity therefore arises by employing the new IR flow cell, as it can be positioned at any point in the reaction stream, to monitor the formation and decay of potentially hazardous reactive intermediates at various points in the reaction sequence down to meaningful detection limits. Of course, monitoring intermediates also allows us to generate information concerning reaction mechanisms.

4.4.1. Curtius Rearrangement. One such example of handling hazardous reactive intermediates safely in flow is the Curtius rearrangement, where an acyl azide rearranges to an isocyanate within the reactor coil which is then intercepted with a nucleophile *in situ* to generate the corresponding amide.[18] The rearrangement reaction was performed according to the previously published protocol using acid **19** (Scheme 7) and placing the IR flow cell between two reactor coils (Figure 15).

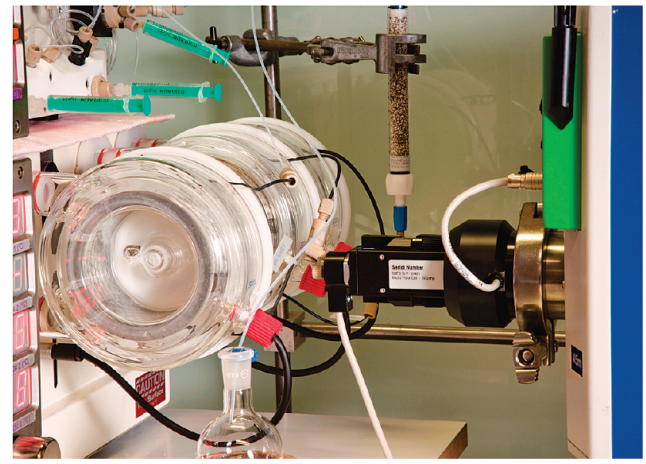

Figure 15. **Setup for monitoring reactive intermediates during the Curtius rearrangement; the IR flow cell is attached between the first and second flow coil.**

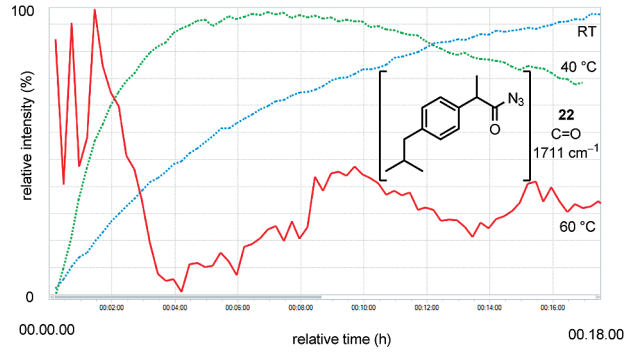

Figure 16. **Trend curves displaying the acyl azide 22 formation at different temperatures during the in-cell optimisation procedure.**

In order to determine an appropriate temperature at which the acyl azide intermediate is stable enough to be monitored, a very rapid in-cell optimization was carried out combining stock solutions of the acid **19**, triethylamine, and azide source DPPA **20** and injecting the mixture into the 51 μL flow cell *via* syringe. The cell was then heated to determine at what rate the acyl azide **22** was formed, and up to which temperature it survives (Figure 16).

Again, the carbonyl peak absorption gave us the best chance of effectively monitoring the acyl azide as it was significantly different to that of the starting acid. As can be seen in Figure 16, the acyl azide intermediate **22** is rapidly formed at 40 °C. At 60 °C it either rearranges immediately to the isocyanate or becomes too unstable to be monitored. In this case we did not see an isocyanate asymmetric N=C=O stretch because this band absorbs in the region blinded by the diamond for this substrate. Having found that 40 °C was an appropriate temperature to monitor the acyl azide **22**, we repeated the reaction with the flow cell mounted between the two CFC coils (Figures 15, 17).

On the first attempt the first coil was heated to 40 °C, and the smooth formation of the acyl azide flowing through the cell was observed as expected. On a second run, the temperature of the first coil was increased to 120 °C (the temperature

(15) Review: Marshall, J. A. *J. Org. Chem.* **2007**, *72*, 8153–8166.
(16) Sakai, D. S.; Lange, H.; Ley, S. V. University of Cambridge, UK. Unpublished work, 2009.
(17) The FlowStart microfluidic reactor is available from FutureChemistry Holding BV, Toernooiveld 100, 6525 EC Nijmegen, The Netherlands. Website: www.futurechemistry.com.
(18) Baumann, M.; Baxendale, I. R.; Ley, S. V.; Nikbin, N.; Smith, C. D.; Tierney, J. P. *Org. Biomol. Chem.* **2008**, *6*, 1577–1586.

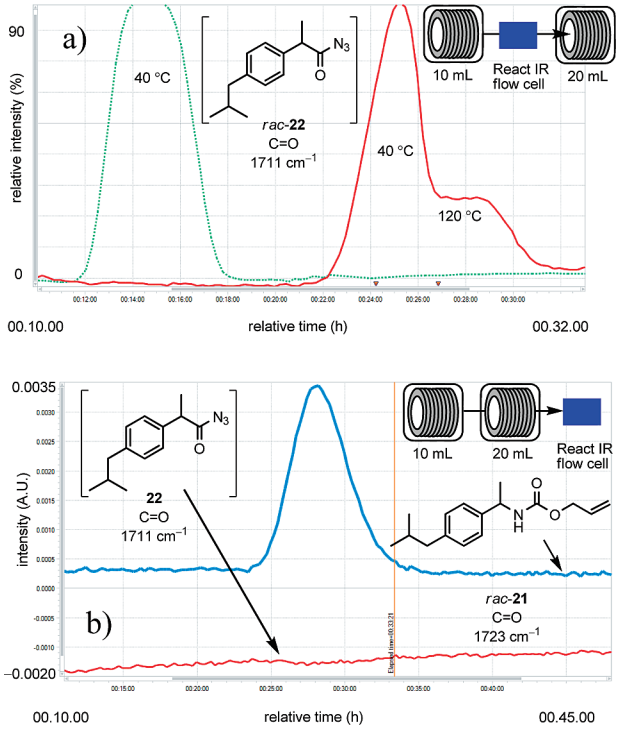

Figure 17. **Monitoring of intermediates (22, (a)) and products (21, (b)) during the Curtius rearrangement.**

Scheme 8. **Generation and monitoring of HN_3 in flow**

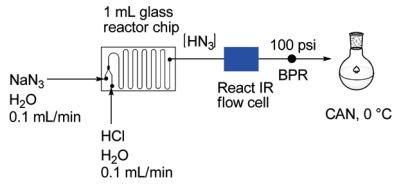

required to cause the desired rearrangement), resulting in the immediate degradation of the azide intermediate **22** as monitored via its band at $\tilde{\nu} = 1711\ cm^{-1}$.

In order to ensure that the reaction was complete the flow cell was then reattached at the end of the two coils to demonstrate that the product is formed under the conditions chosen by tracking the dispersion curve of the amide band of the product **21** at $\tilde{\nu} = 1723\ cm^{-1}$. A double-headed flow cell, which will allow the simultaneous evaluation of reactive intermediates and product formation, has recently become available.[12]

4.5. Monitoring Hazardous Waste Materials. *4.5.1. Azide Monitoring.* Inspired by another ongoing project within our group[19] we investigated whether the new IR flow cell could be used as an analytical tool for the inline monitoring of hazardous byproducts, in particular HN_3, as this can be formed from $TMSN_3$ as an intermediate during the acidic inline workup of reactions.[20] Therefore, HN_3 was deliberately generated from sodium azide and hydrochloric acid on a small scale *in situ* so as to obtain a library spectrum (Scheme 8).

Again, due to the blackout region of the cell caused by the diamond absorption, the corresponding symmetric N═N stretch

(19) Smith C. J.; Nikbin, N.; Smith, C. D.; Ley, S. V.; Baxendale, I. R. *Org. Biomol. Chem.* **2010**, *8*. Manuscript in preparation.

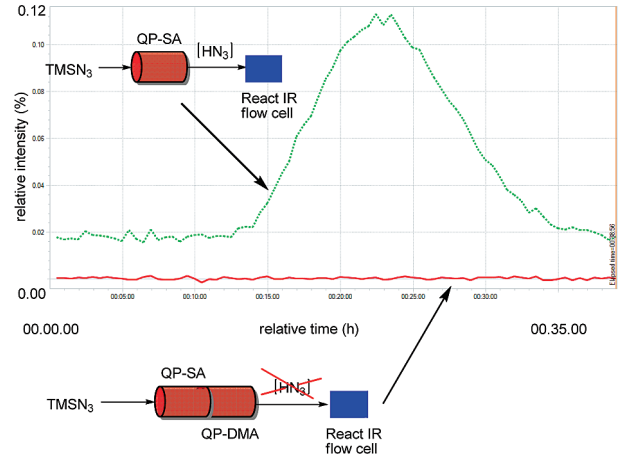

Figure 18. **Monitoring generation (upper equation) vs generation and subsequent scavenging (lower equation) of HN_3 in flow (QP-SA: polymer-supported sulfonic acid; QP-DMA: polymer-supported trimethylamine).**

at $\tilde{\nu} = 1175\ cm^{-1}$, rather than the stronger absorbing asymmetric stretch, was used as the monitoring band.

With the information from the control reaction in hand we then set out to determine if $TMSN_3$ could be safely scavenged inline by purposefully passing it through a column of supported acid and flowing the exiting HN_3-containing stream through a column of supported base to scavenge it as a polymer-supported salt (Figure 18). Indeed, on passage of $TMSN_3$ through an acidic column the symmetric N═N stretch for $TMSN_3$ at $\tilde{\nu} = 1255\ cm^{-1}$ was not observed any more; instead the HN_3 band appeared at $\tilde{\nu} = 1175\ cm^{-1}$, indicating that HN_3 had indeed been formed. By repeating this procedure and by additionally adding the previously mentioned downstream base column to the reaction line, no azide residues were detected within the exiting solution.

This result demonstrates that the flow cell could be very useful as a monitoring device for analysis of potentially contaminated azide waste streams.[21] With the silicon cell being manufactured[12] the sensitivity of this monitoring process will be greatly increased as the strong absorption of the major azide asymmetric stretch around $\tilde{\nu} = 2100\ cm^{-1}$ will be clearly visible allowing much lower concentrations to become detectable.

4.6. Monitoring Batch reactions. Having successfully addressed several important issues connected with flow chemistry, we wanted to finally demonstrate the *general* applicability of the IR flow cell by using it for real-time analysis of small-scale batch processes, since the more cumbersome fibre-optic probe alternative is a much less convenient choice here. In order to make use of the new flow cell for these reactions, we designed a reaction setup as depicted in Figure 19. Here a

(20) Issues could potentially arise when the diamond-based ATR IR flow cell is used for monitoring azide chemistry, as some azide species are not compatible with the gold seal that is currently employed. However, we did not see any damage of that gold seal while operating the system for azide monitoring as described. We assume that the low concentrations of aggressive azide species were beneficial in this case. Alternative types of seals are available upon request if necessary.

(21) For azide detection down to concentrations of 0.005 M using ferric(III) chloride solution, see: (a) Reference 15 in: Kopach, M. E.; Murray, M. M.; Braden, T. M.; Kobierski, M. E.; Williams, O. L. *Org. Process Res. Dev.* **2009**, *13*, 152–160. (b) Feigl, F.; Anger, V.; Oesper, R. E. *Spots in Inorganic Analysis*, 6th ed.; Elsevier Publishing Company: Amsterdam, London, NY, 1972.

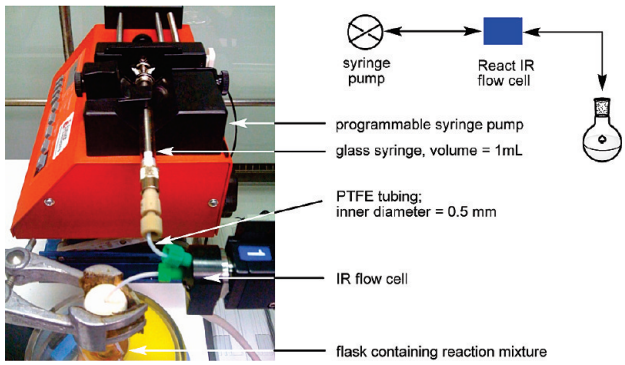

Figure 19. **Setup for the FT-IR analysis of batch reactions using the flow cell.**

Scheme 9. **Peptide coupling reaction using batch conditions**

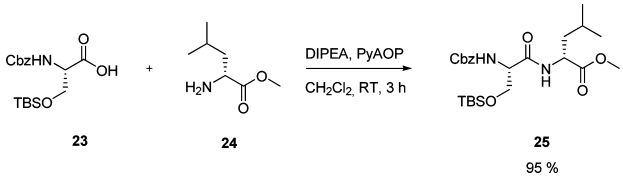

commercially available, programmable syringe pump[22] was used to sequentially withdraw and reinject 200 μL of the stirred reaction mixture through the flow cell. In order to ensure a minimum dead volume in the linking flow tubes, very fine dimensioned (inner diameter = 0.5 mm) PTFE tubing was used, thereby keeping the connections as short as possible. A fairly high pumping rate was also programmed in order to ensure a fast "loading" of the cell. An interval of one minute was chosen between the two pumping events, and the solution was scanned every 30 s for the IR profile. This arrangement ensured a reliable monitoring of the processes occurring in the flask over time.

4.6.1. Peptide Coupling Reaction in Batch. To illustrate the versatility of this unconventional arrangement a peptide coupling reaction was chosen as it involves a complex mixture of reagents, intermediates, product, and byproduct and as it often requires extensive substrate-dependent optimisation to render it efficient in terms of time management (Scheme 9).[23]

By using the setup depicted, the reaction was successfully monitored (Figure 20). It was once more possible to distinguish between the different carbonyl functions of the leucine substrate **24**, intermediate active ester **26**, and the desired dipeptide **25** that formed slowly over the course of the experiment (Figure 20). When the coupling reagent, PyAOP, was added, an immediate formation of the intermediate active ester **26** can be seen; this line appears to persist throughout the reaction because there is some overlap with the band corresponding to the newly formed product ester **25**. The product forms as the active ester **26** decays, so the overall sum of amounts contributing to the peak level remains constant, resulting in a nearly horizontal trend line. In this case, the three-dimensional surface analysis of the second derivative spectrum implemented into the software greatly assisted in the assignment and the outlined interpretation,

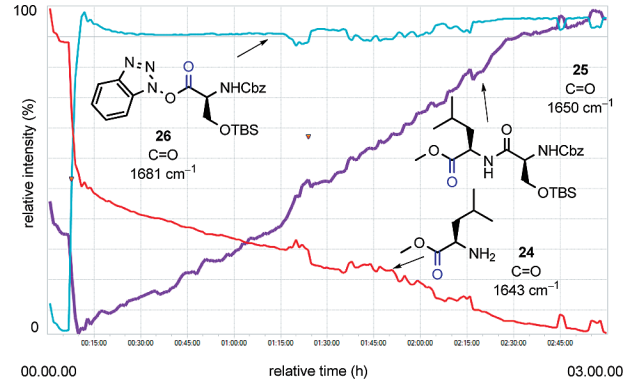

Figure 20. **Trend analysis (second derivatives) for substrate ester 24, intermediate activated ester 26, and product amide 25.**

as the active ester **26** decaying as the product ester **25** peak increases is more clear (Figure 21).

5. Conclusions

In conclusion we have reported the wide utility of the new ReactIR flow cell for micro- and mesofluidic continuous flow chemistry processing applications. With the use of this device it was possible to monitor a variety of important functionalities present in organic molecules such as C=O, C=C (although hard to distinguish from noise in lower concentrations), C=N, N_3, C−F, and C−O and also to visualize reactive reaction intermediates in real time and down to concentrations of 0.05 M. This new equipment should find many new applications by providing structural information which facilitates reaction optimisation and which would generate new knowledge of reaction pathways.

6. Experimental Details

General Remarks. Acetonitrile and methylene chloride were dried over calcium hydride and distilled prior to use. Tetrahydrofuran was dried according to the Grubb's protocol.[24] Ethanol and methanol were used as purchased without further purification. All reagents were used as purchased without further purification. ^{1}H NMR spectra were recorded at 27 °C on a Bruker DPX-400. Residual protic solvent was used as the internal reference ($CHCl_3$ δ_H = 7.27 ppm). ^{13}C NMR spectra were recorded at 100 MHz on Bruker DPX-400. Coupling constants are quoted to the nearest 0.1 Hz. Multiplicities are abbreviated as follows: s - singlet, d - doublet, t - triplet, q - quartet, m - multiplet, br - broad, dd - doublet of doublets, etc. The resonance $CDCl_3$ (δ_C = 77.0 ppm, t) was used as the internal reference. Mass spectra were recorded on Waters LCT Premier, Bruker Daltronics Bioapex II or Kratos Concept spectrometers. Accurate mass data were obtained on Micromass Q-TOF by electrospray ionisation (ESI). Conventional infrared spectra were recorded neat on a Perkin-Elmer Spectrum One FT-IR spectrometer using Universal ATR sampling accessories. Optical rotations were measured on a Perkin-Elmer model 343 digital polarimeter at 25 °C.

Fluorination Reactions. The procedure outlined in ref 10 was used with the IR flow cell attached inline just before the back-pressure regulator as the only alteration.

(22) An NE-1000 single-syringe pump was used which is available from New Era Pump System, Inc., 2517 Bayview Ave., Wantagh, New York 11793−4305, U.S.A. Website: www.syringepump.com.

(23) Kumarn, S.; Hoffmann, T. J.; Ley, S. V. University of Cambridge, UK. Unpublished work, 2009.

(24) Pangborn, A. B.; Giardello, M. A.; Grubbs, R. H.; Rosen, R. K.; Timmers, F. J. *Organometallics* **1996**, *15*, 1518–1520.

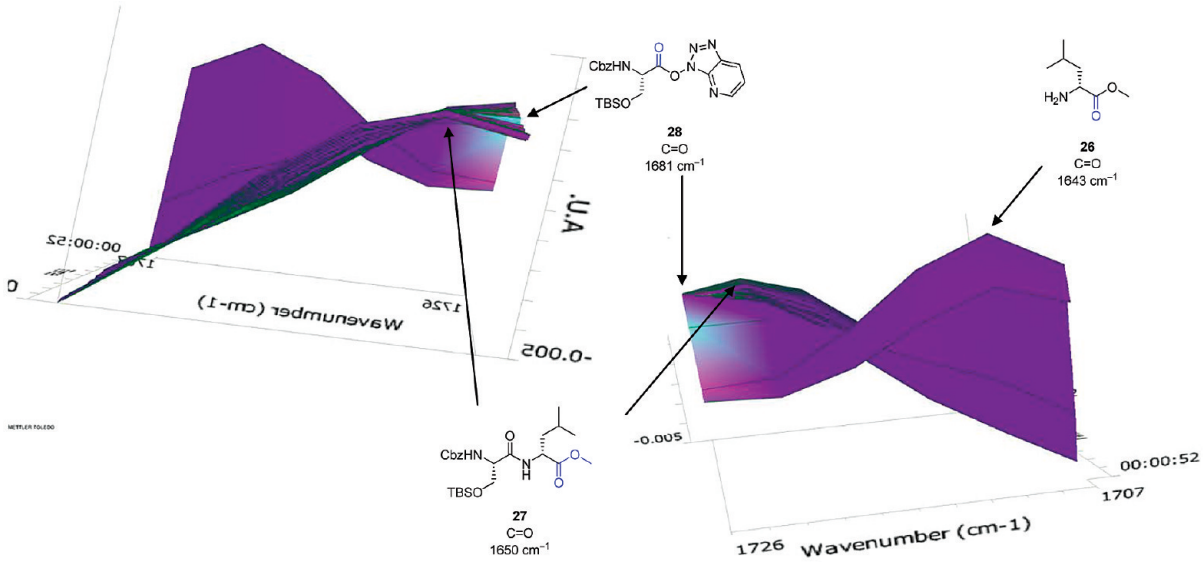

Figure 21. **Three-dimensional plots of the peak surface obtained in the peptide coupling reaction (view from the "front" in the direction of the relative reaction time (right) and from "behind" in the direction of the negative relative reaction time (left).**

2-Chloro-3-(difluoromethyl)-6-methoxyquinoline (3). Analytical data are in agreement with previously published data.[10b]

1-(Difluoromethoxy)-4-nitrobenzene (5). Using the standard setup, the product was formed in 60% conversion (^{1}H NMR of crude product mixture). Upon purification using column chromatography on silica gel, partial decomposition was observed. Further optimizations are currently being undertaken; full analytical data pending.[10b] Colourless oil, ^{1}H NMR (400 MHz, $CDCl_3$) δ/ppm: 6.63 (1H, t, $J_{H-F} = 72.3$ Hz, CF_2H), 7,26 (2H, dd, $J = 9.2$ Hz, $J = 2.4$ Hz, Ar-*H*), 8.72 (2H, dd, $J = 9.2$ Hz, $J = 2.4$ Hz, Ar-*H*).

Oxazole Formation. The procedure outlined in reference[11] was used with the IR flow cell put inline just before the back-pressure regulator as the only alteration.

5-(3-Nitrophenyl)oxazole-4-carboxylic Acid Ethyl Ester (8). Analytical data are in agreement with previously published data.[11]

Hydrogenation Reactions. The general arrangement as described earlier in references[4i,8a] for doing recycling hydrogenation reactions in flow was used, with the only alterations being the IR flow cell attached inline in between the vessel containing the substrate/product mixture and the pump (compare with the schematic drawing in Figure 8, Scheme 5).

Methyl Piperidine-3-carboxylate (8). Methyl nicotinate (4.89 g, 35.6 mmol) was dissolved in 350 mL of a 4:6 mixture of ethanol and water. The recycling process was run using the H-Cube Midi with 5 mL/min through a MidiCart containing 5% Pd/C at 90 °C and 80 bar. After 200 min the reaction was stopped. A sample of the reaction mixture was taken for ^{1}H NMR analysis, displaying 90% conversion. Analytical data are in agreement with previously published data.[14b]

(2R,3S,5R,6R)-Dimethyl 5,6-Dimethoxy-5,6-dimethyl-1,4-dioxane-2,3-dicarboxylate (12). (5*R*,6*R*)-Dimethyl 5,6-dimethoxy-5,6-dimethyl-5,6-dihydro-1,4-dioxine-2,3-dicarboxylate (300 mg, 1.0 mmol) was dissolved in 10 mL of methanol. The recycling process was run using the H-Cube with 1 mL/min through a CatCart containing 5% Rh/Al_2O_3 at 40 °C and 60 bar. After 4 h the reaction was stopped. A sample of the reaction mixture was taken for ^{1}H NMR analysis, revealing the conversion of 70%. Analytical data for fully converted sample:[8b] Colourless solid, mp: 100−102 °C. $[\alpha]_D^{25} = -95.5$ ($c = 0.66$, $CHCl_3$). ^{1}H NMR (400 MHz, $CDCl_3$) δ/ppm: 1.33 (3H, s, CCH_3), 1.38 (3H, s, CCH_3), 3.21 (3H, s, $COCH_3$), 3.30 (3H, s, $COCH_3$), 3.75 (3H, s, CO_2CH_3), 3.77 (3H, s, CO_2CH_3), 4.50 (1H, d, $J =$ 3.8 Hz, C*H*), 4.69 (1H, d, $J = 3.8$ Hz, C*H*). ^{13}C NMR (100 MHz, $CDCl_3$) δ/ppm: 17.3 (CCH_3), 17.8 (CCH_3), 48.4 ($COCH_3$), 50.1 ($COCH_3$), 51.9 (CO_2CH_3), 52.1 (CO_2CH_3), 66.1 (*C*H), 69.1 (*C*H), 99.3 (*C*), 100.4 (*C*), 168.8 (*C*O), 169.6 (*C*O). IR (ATR) $\tilde{\nu}$/cm^{-1}: 2954, 1770, 1736, 1140, 1034. HRMS (ESI) *m*/*z*: Calcd for $C_{12}H_{20}NaO_8$ ($M + Na^+$): 315.1056. Found: 315.1074.

Butane-2,3-diacetal Protection Reaction. A solution of (*R*)-chloropropanediol (2,00 g, 18.0 mmol) and CSA (417 mg, 1.80 mmol) in 5 mL of methanol and another solution of butanedione (1.93 mL, 22.0 mmol) and trimethyl orthoformate (4.38 mL, 40.0 mmol) in 5 mL of methanol were prepared. Using the Vapourtec R2+/R4 system, the solutions were pumped at a flow rate of 0.15 mL/min into a CFC reactor heated at different temperatures. The solution was then passed through a 10 mm × 300 mm OmniFit column filled with QP-BZA resin (2 g) and the output collected. The product formed at 90 °C was collected, and the solvent was removed *in vacuo* to obtain the desired material. The yield was not determined.

The 24 h scale-up experiment afforded dioxane **15** in 88% yield.

(2R,3R)-5-(Chloromethyl)-2,3-dimethoxy-2,3-dimethyl-1,4-dioxane (15). Colourless oil, $[\alpha]_D^{25} = -101.3$ ($c = 0.8$, $CHCl_3$). ^{1}H NMR (400 MHz, $CDCl_3$) δ/ppm: 1.28 (3H, s, CH_3), 1.30 (3H, s, CH_3), 3.26 (3H, s, OCH_3), 3.29 (3H, s, OCH_3), 3.38 (1H, dd, $J = 11.3$, 6.2 Hz, CH*H*Cl), 3.43 (1H, dd, $J = 11.3$, 6.2 Hz, C*H*HCl), 3.62−3.58 (2H, m, OCH_2), 4.08 (1H, ddd, $J = 11.3$, 9.2, 6.2 Hz, C*H*). ^{13}C NMR (100 MHz, $CDCl_3$) δ/ppm:

17.2 (CCH_3), 17.4 (CCH_3), 47.7 (OCH_3), 47.8 (OCH_3), 61.3 (CH_2Cl), 67.3 (*C*H), 97.9 (*C*), 99.2 (*C*). IR (ATR) $\tilde{\nu}$/cm^{-1}: 2948, 1374, 1114, 1035, 878. HRMS (ESI) *m*/*z*: Calcd for $C_9H_{17}ClNaO_4$ (M + Na^+): 247.0713. Found: 247.0733.

Addition of Allenylstannanes to Aldehydes in Flow. A solution of cyclohexylcarbaldehyde (24 mg, 0.2 mmol) in 2.0 mL of methylene chloride and another solution of *rac*-buta-1,2-dienyltributylstannane (24 μL, 0.2 mmol) and bortrifluoride etherate (49 μL, 0.4 mmol) in 2.0 mL of methylene chloride were prepared. Using the FutureChemistry FlowStart microfluidic arrangement,[17] the solutions were mixed in a 10 μL glass chip at different temperatures and with different flow rates for screening purposes, yielding the desired product in different diastereomeric ratios (determined by ^{1}H NMR analysis of the crude product) and in different yields.[15] The material obtained under optimised conditions[15] was collected, the solvent was removed *in vacuo*, and the crude product mixture was finally subjected to column chromatography on silica gel to obtain analytical data.

syn-1-Cyclohexyl-2-methylbut-3-yn-1-ol (syn-18): colourless oil, R_f = 0.34 (hexane/Et_2O = 10:1). ^{1}H NMR (400 MHz, $CDCl_3$) δ/ppm: 0.99−1.34 (12H, m, Cyclohexyl-*H*), 1.20 (3H, d, J = 6.9 Hz, CH_3) 1.50−1.79 (5H, m, Cyclohexyl-*H*), 1.93−1.96 (1H, bs, Cyclohexyl-*H*), 2.11 (1H, d, J = 2.4 Hz, C≡C*H*), 2.62−2.69 (1H, m, $CHCH_3$), 3.36 (1H, dd, J = 10.3, 5.6 Hz, C*H*OH). Analytical data are in agreement with previously published data.[25]

Curtius Rearrangement Reaction. The procedure outlined in reference 18 was used with the IR flow cell put inline just before the back-pressure regulator in order to monitor the product formation or inline after the first 10 mL CFC reactor as the only alterations.

Allyl-1-(4-isobutylphenyl)ethyl Carbamate (21). Analytical data are in agreement with previously published data.[18]

Azide Monitoring in Flow. Generation of HN_3 in flow: 0.125 M standard solutions of HCl and NaN_3 in water were prepared and injected into two 2 mL sample loops attached to the Vapourtec R2+/R4. The solutions were mixed at a flow rate of 0.1 mL/min per pump through a 1 mL glass chip and through the IR flow cell before being poured into a concentrated solution of CAN in water at 0 °C.[26]

Alternatively, a standard solution of $TMSN_3$ (1 M) in CH_3CN was prepared. This was then loaded in a sample loop and subsequently pumped at a rate of 0.2 mL/min through an OmniFit glass column filled with QP-SA (one-third) and QP-DMA (two-thirds) or QP-SA only, respectively, before quenching by pouring into a concentrated solution of CAN in water at 0 °C.[26]

Peptide Coupling Reactions. To a stirred solution of *Z*-L-serine (TBS)−OH[27] (500 mg, 1.42 mmol) in THF (4.5 mL) was added D-leucine methyl ester (205 mg, 1.42 mmol), followed by DIPEA (0.75 mL, 4.25 mmol). The resulting solution was cooled to 0 °C before adding PyOAP (782 mg, 2.13 mol). During the reaction time, 200 μL of the reaction mixture was withdrawn through the IR flow cell into a 1 mL glass syringe by a programmable syringe pump (0.75 mL/min). One minute after the withdrawal process started, a reinjection process was started delivering the 200 μL back into the solution (0.75 mL/min). This procedure was run during the whole reaction time. The IR flow cell was connected to the flask and to the syringe pump by PTFE tubing (inner diameter 0.5 mm, total length of tubing used: 15 cm) using OmniFit connections. After stirring at RT for 3 h both amino acids were completely consumed (IR and TLC). The reaction mixture was quenched with water (10 mL) and extracted with EtOAc (3 × 10 mL). The combined organic phases were dried over $MgSO_4$, filtered, and concentrated *in vacuo*. Purification by flash column chromatography (100:0 → 50:1 → 10:1 → 3:1 light petrol/EtOAc) provided the desired dipeptide (651 mg, 95%).

(R)-Methyl 2-((S)-2-(Benzyloxycarbonylamino)-3-(tert-butyldimethylsilyloxy)propanamido)-4-methylpentanoate (25): colourless solid, R_f = 0.61 (light petrol/EtOAc = 2:1), mp: 93−94 °C. $[\alpha]_D^{25}$ = +23.4 (c = 1.13, $CHCl_3$). ^{1}H NMR (400 MHz, $CDCl_3$) δ/ppm: 0.08 (3H, s, $Si(CH_3)(CH'_3)$), 0.09 (3H, s, $Si(CH_3)(CH'_3)$), 0.89 (9H, s, $SiC(CH_3)_3$), 0.91 (3H, d, J 6.2, $CH_2CH(CH_3)(CH'_3)$), 0.92 (3H, d, J 6.2, $CH_2CH(CH_3)(CH'_3)$), 1.48−1.57 (1H, m, $CHH'CH(CH_3)_2$), 1.59−1.67 (2H, br m, $CHH'CH(CH_3)_2$), 3.66 (1H, dd, J 9.8, 7.3, $CHH'OSi$), 3.71 (3H, s, OCH_3), 4.05 (1H, br dd, J 9.8, 3.6, $CHH'OSi$), 4.18−4.24 (1H, br m, $CHCH_2OSi$), 4.65 (1H, td, J 8.7, 5.1, $CHCH_2CH(CH_3)_2$), 5.10 (1H, d, J 12.2, $OCHH'Ph$), 5.15 (1H, d, J 12.2, $OCHH'Ph$), 5.64−5.72 (1H, br m, $NHCOOCH_2Ph$), 6.86 (1H, br d, J 5.1, $CONHCHCOOCH_3$), 7.28−7.36 (5H, m, 5 × Ph*H*). ^{13}C NMR (100 MHz, $CDCl_3$) δ/ppm: −5.6 and −5.5 ($Si(CH_3)_2$), 18.1 ($SiC(CH_3)_3$), 21.9 and 22.7 ($CH_2CH(CH_3)_2$), 24.7 ($CH_2CH(CH_3)_2$), 25.7 ($SiC(CH_3)_3$), 41.7 ($CH_2CH(CH_3)_2$), 50.8 ($CHCH_2CH(CH_3)_2$), 52.2 ($COOCH_3$), 55.8 ($CHCH_2OSi$), 63.2 (CH_2OSi), 67.1 (OCH_2Ph), 128.1, 128.2, and 128.5 (5 × Ph*C*), 136.2 (Ph*C*-ipso), 156.0 ($NCOOCH_2Ph$), 169.7 ($CONHCHCOOCH_3$), 172.9 ($COOCH_3$). IR (film) $\tilde{\nu}$/cm^{-1}: 3287, 2958, 2928, 2856, 1733, 1691, 1646, 1541, 1468, 1398, 1307, 1276, 1244, 1120, 1051, 1005, 939, 837, 776, 738, 694. HRMS (ESI) *m*/*z*: Calcd for $C_{24}H_{40}N_2O_6Si$ (M + H^+): 481.2734. Found: 481.2739.

Acknowledgment

We thank AstraZeneca (C.F.C.), the Alexander von Humboldt Foundation (H.L.), the EPSRC (I.R.B, H.L.) and the Royal Society (I.R.B) for funding, and the BP Endowment (S.V.L).

Received for review November 17, 2009.

OP900305V

(25) Danheiser, R. L.; Carini, D. J.; Kwasigroch, C. A. *J. Org. Chem.* **1986**, *51*, 3870–3878.

(26) For the destruction of azides using ceric ammonium nitrate solution, see: Armour, M.-A. *Hazardous Laboratory Chemicals Disposal Guide*, 3rd ed.; CRC Press LLC: Boca Raton, Florida, U.S.A., 2003; p 461.

(27) Prepared according to Deeley, J.; Bertram, A.; Pattenden, G. *Org. Biomol. Chem.* **2008**, *6*, 1994–2010.